Ultrahigh-resolution optical imaging of colloidal particles

2002 J. Phys.: Condens. Matter 14 7749

(http://iopscience.iop.org/0953-8984/14/33/313)

INSTITUTE OF PHYSICS PUBLISHING JOURNAL OF PHYSICS: CONDENSED MATTER

J. Phys.: Condens. Matter **14** (2002) 7749–7756 PII: S0953-8984(02)39326-3

Ultrahigh-resolution optical imaging of colloidal particles

Roy Pike[1] **and Shi-Hong Jiang**[2,3]

[1] Department of Physics, King's College, Strand, London WC2R 2LS, UK
[2] Department of Fine Mechanical Engineering, Shanghai University, Shanghai, People's Republic of China

E-mail: erp@maxwell.ph.kcl.ac.uk (Roy Pike)

Received 10 July 2002
Published 9 August 2002
Online at stacks.iop.org/JPhysCM/14/7749

Abstract

We continue the theme exploited very effectively by Professor Pusey over the years of using laser light to measure the size of colloidal particles. A description of a new measurement technique using a confocal scanning laser microscope (CSLM) is given in which the Rayleigh resolution limit of a numerical aperture 1.3 oil-immersion objective is effectively doubled. The method exploits the 'natural' bandwidth of an imaging system with a very low number of 'degrees of freedom' (generalized Shannon number) which is realized in the CSLM by using the high-aperture objective lens both to illuminate the particles and to collect the scattered light from them. The available extra resolution is not visible in the conventional recorded image of the instrument and the full double-bandwidth 'information' content in the image plane is extracted in our method by using a specially calculated optical mask as an instantaneous analogue computer. We have modified a commercial Bio-Rad 600 confocal microscope to work in this way and present here the first measurements obtained with it. We compare images of 100 nm diameter standard PVC fluorescent calibration spheres with the new and the older modalities. The results confirm the expected increase in optical resolution.

1. Introduction

The science of colloidal particles has had a long evolving history and is of importance in many diverse areas of application. With 'nanoscience' moving to centre stage in modern physical research, the subject seems now to be of ever increasing importance, particularly with new surface stabilization methods which allow novel optical properties to be exploited. The dedicatee of this special issue, Peter Pusey, has contributed significantly to this field over several decades. As is well known, he has been a pioneer in the application of laser light scattering to investigate physical properties of colloidal particles and the interactions between

[3] Present address: Department of Electrical Engineering, University of Nottingham, Nottingham, UK.

them. These light scattering techniques are now of great value in experimental colloid science and a number of commercial light scattering instruments are available.

One of these important properties is particle size. In this contribution we present ultrahigh-resolution optical images of colloidal particles using a new modality of operation of a high-numerical-aperture confocal scanning laser microscope (CSLM) in which the Rayleigh resolution limit of the microscope objective can be effectively doubled. Of course the new modality can be used for fluorescence microscopy in other disciplines, with the same increase in resolving power, and we are at present also obtaining our first images of biological specimens, which will be published elsewhere.

In a confocal scanning microscope [1] the object is illuminated by a raster-scanned focused beam and the transmitted, reflected or fluorescent light which passes through a pinhole at the centre of the image plane is then detected. Imaging systems can be allocated [2] an information theoretic, noise-dependent 'generalized Shannon number', or number of degrees of freedom, which can be used to determine the optical resolution limit. In this approach the conventional image is regarded merely as experimental data from which the actual image must be calculated. As we shall see, this calculation may be done optically by use of a suitable image-plane mask. The new method takes account of the fact that the spatial-frequency response of the imaging operator of the CSLM system essentially completely fills a band of twice the width of that of the objective lens.

2. Theory of the optical mask

In a series of earlier theoretical papers on optical imaging (for references see, for example, [3]) we have shown that when focused beams are used for illumination with either coherent or incoherent light and at all numerical apertures, the conventional theory of optical resolution, including confocal scanning, underestimates the correct diffraction limit and that a suitably designed system can robustly achieve an increase in linear resolution approaching twice the Rayleigh criterion.

These developments are based on work over recent years with the group of Professor Bertero at the University of Genoa and other colleagues and uses the techniques of the inter-disciplinary field of 'inverse problems' (see, for example, the well-established journal *Inverse Problems* published by the Institute of Physics in the UK). In fact, our original introduction to this field was motivated by the need to invert light scattering data of the type mentioned above.

Linear inverse problems, of which optical imaging is an example, are described by Fredholm integral equations of the first kind (in some discretized form), which relate experimental data to their physical interpretation. One attempts to quantify the 'information content' of the data using a generalized form of Shannon's information theory [2]. For example, apart from its application to optical imaging, we have used similar mathematical approaches to make progress in other fields of modern theoretical physics such as high-temperature superconductivity [4] and the design of radar and sonar antennas [5].

Much of our earlier work in optical imaging was devoted to establishing these principles of 'superresolution' in low-aperture optical systems where the calculations could, for the most part, be done analytically. More recently, with the advent of sufficiently powerful computers, we have been able to handle the computations required for high-aperture systems, both incoherent and coherent. For example, with the collaboration of the Philips optical storage group, in a European Union project acknowledged below, we are attempting to apply solutions in the coherent case to the problem of increasing optical storage densities of DVDs.

In the application of the methods of inverse problems to scanning imaging systems one considers the image plane to contain 'data' which must be used to determine as much

information as possible about the object which generated it. It is also made clear that this information, in general, cannot be used to reconstruct the input completely since, as we shall see in a moment, the mathematical operator which transforms the input into the data is linear and compact and is thus a 'smoothing' operator.

The theory shows that there is a 'natural' basis for each such operator which provides a complete set of orthonormal components in which to expand the input and output (not necessarily the same for both) which are ordered in such a way that the components which are most robust to noise interference are those with the lower indices which, as in a Fourier expansion, are those which vary less rapidly. A generalized, noise-dependent 'Shannon number' can be defined, which is the index which limits the so-called 'signal subspace'. Without further *a priori* information the noise prevents reliable recovery of the components with indices higher than this value, which will reside in the 'noise subspace', unless present in inordinate strength. This gives rise to a defined 'resolution' limit. We may note here however that we have found [6], perhaps surprisingly, that if the input is known to be positive all these higher components can, in fact, be recovered by using the further assumptions of a minimum-L^2-norm, positive solution. We have not yet applied this result to the present problem.

The process of reconstruction of the object in a scanning optical system using these concepts can be effected by placing a specially calculated, generally complex, optical mask in the image plane and integrating the transmitted and/or reflected amplitudes using suitable collection optics [7].

We will give a brief outline of the definition and calculation of an image-plane mask for a generic imaging operator, A, defined by

$$(Af)(y) = \int A(x, y) f(x)\, \mathrm{d}x \tag{1}$$

where x and y can be multi-dimensional. We call the object $f(x)$ and the image $g(y)$ and the imaging is described by the operator equation

$$g = Af. \tag{2}$$

The image-plane mask is calculated using the singular-value decomposition (SVD) of the operator A, which we consider in the first place to act upon square integrable functions, i.e. it maps functions from one L^2-space into another. The SVD is given by the set of solutions $\{\alpha_k; u_k, v_k\}_{k=0}^{\infty}$ of the coupled integral equations

$$Au_k = \alpha_k v_k, \qquad A^* v_k = \alpha_k u_k, \tag{3}$$

where A^* denotes the adjoint of A. The u_k and v_k are called singular functions and provide orthonormal bases for f and g, respectively. The α_k are called singular values and for a compact operator A they accumulate to zero with increasing k; they represent the strength with which each component is transferred into the image and hence how well it can withstand the addition of noise. SVD can be accomplished using standard numerical packages found in many software libraries.

Given this decomposition of the imaging operator, by expanding object and image in their respective bases and using their orthonormality it can be seen after a little algebra that the solution of (2) is

$$f(x) = \sum_{k=0}^{\infty} \frac{1}{\alpha_k} u_k(x) \int g(y) v_k(y)\, \mathrm{d}y \tag{4}$$

and specifically, on the optical axis,

$$f(0) = \sum_{k=0}^{\infty} \frac{1}{\alpha_k} u_k(0) \int g(y) v_k(y)\, \mathrm{d}y. \tag{5}$$

For a scanning system the determination of $f(0)$ at each point of the scan is sufficient to reconstruct the image. Exchanging the sum in (5) with the integral we obtain

$$f(0) = \int g(y)M(y)\,\mathrm{d}y, \tag{6}$$

where

$$M(y) = \sum_{k=0}^{\infty} \frac{1}{\alpha_k} u_k(0)v_k(y). \tag{7}$$

The function $M(y)$ is called an image-plane optical mask and it can be seen that (6) explains the object reconstruction process described earlier. In practice the summation is truncated at a value of k which depends on the signal-to-noise ratio of the detected signal. Using the fact that (6) is the scalar product (M, g) in L^2 of M and g and that $g = Af$, we can see that

$$f(0) = (M, g) = (M, Af) = (A^*M, f). \tag{8}$$

Thus we can write

$$f(0) = \int T(x)f(x)\,\mathrm{d}x, \tag{9}$$

where T is given by

$$T = A^*M. \tag{10}$$

3. The imaging equation of a high-aperture confocal scanning system

Let us consider a three-dimensional fluorescent object and denote the distribution function of its fluorescent centres by $f(\boldsymbol{\rho}; z)$ where z is the coordinate along the optic axis and $\boldsymbol{\rho}$ is a radial vector perpendicular to it. For fluorescence microscopy, circularly polarized light can be used and circular symmetry imposed. Under some reasonable assumptions [3], which we will not detail here, the basic imaging equation of the scanning confocal microscope gives the intensity distribution in the image plane as

$$g(\boldsymbol{\rho}) = \int W_2(|\boldsymbol{\rho} - \boldsymbol{\rho}'|; z')W_1(|\boldsymbol{\rho}'|; z')f(\boldsymbol{\rho}'; z')\,\mathrm{d}\boldsymbol{\rho}'\,\mathrm{d}z', \tag{11}$$

where $W_1(|\boldsymbol{\rho}|; z)$ and $W_2(|\boldsymbol{\rho}|; z)$ are the rotationally symmetric point spread functions (PSFs) (i.e. the time-averaged energy distributions in the focal region), respectively, of the illuminating lens and the imaging lens. We shall consider here the confocal microscope working in the epifluorescence mode with a single unaberrated lens, of opening semi-angle α, used both for illumination and imaging, so that

$$W_1(\rho; z) = W_2(\rho; z) \equiv W(\rho; z). \tag{12}$$

For lenses with high numerical apertures, we must use the full expression for the PSF $W(\rho; z)$, derived first in [8] as

$$W(\rho; z) = |I_0(\rho; z)|^2 + 2|I_1(\rho; z)|^2 + |I_2(\rho; z)|^2, \tag{13}$$

where

$$I_0(\rho; z) = \int_0^{\alpha} \sqrt{\cos\theta}\,\sin\theta(1 + \cos\theta)J_0\left(\frac{\sin\theta}{\sin\alpha}\rho\right)\exp\left\{\mathrm{i}\frac{\cos\theta}{\sin^2\alpha}z\right\}\mathrm{d}\theta, \tag{14}$$

$$I_1(\rho; z) = \int_0^{\alpha} \sqrt{\cos\theta}\,\sin^2\theta J_1\left(\frac{\sin\theta}{\sin\alpha}\rho\right)\exp\left\{\mathrm{i}\frac{\cos\theta}{\sin^2\alpha}z\right\}\mathrm{d}\theta, \tag{15}$$

$$I_2(\rho; z) = \int_0^{\alpha} \sqrt{\cos\theta}\,\sin\theta(1 - \cos\theta)J_2\left(\frac{\sin\theta}{\sin\alpha}\rho\right)\exp\left\{\mathrm{i}\frac{\cos\theta}{\sin^2\alpha}z\right\}\mathrm{d}\theta. \tag{16}$$

The most important property of $W(\boldsymbol{\rho}; z)$ is that its Fourier transform

$$\hat{W}(\boldsymbol{\omega}; \eta) = \int_{\mathbb{R}^3} W(\boldsymbol{\rho}; z) \exp[-\mathrm{i}(\boldsymbol{\rho}\boldsymbol{\omega} + \eta z)] \, \mathrm{d}\boldsymbol{\rho} \, \mathrm{d}z \tag{17}$$

$$= 2\pi \int_0^{+\infty} \rho \, \mathrm{d}\rho \int_{-\infty}^{+\infty} \mathrm{d}z \, J_0(\omega\rho) \mathrm{e}^{-\mathrm{i}\eta z} W(\rho, z), \tag{18}$$

where $\boldsymbol{\omega} = (\omega_1, \omega_2)$ is bounded, with support contained within a cylinder

$$|\boldsymbol{\omega}| \leqslant \Omega_\perp, \qquad |\eta| \leqslant \Omega_\parallel, \tag{19}$$

where

$$\Omega_\perp = 2\pi, \qquad \Omega_\parallel = \frac{\pi}{1 + \cos\alpha}. \tag{20}$$

It can be shown that $\hat{g}(\boldsymbol{\omega})$ has its support in the circle $|\boldsymbol{\omega}| \leqslant \Omega_\perp$ and that $\hat{f}(\boldsymbol{\omega}; \eta)$ has its support in the cylinder $|\boldsymbol{\omega}| \leqslant 2\Omega_\perp$, $|\eta| \leqslant 2\Omega_\parallel$. Using these properties it can be demonstrated that the integral operator $\boldsymbol{A}$ of (11) is of the Hilbert–Schmidt class and therefore is compact. Thus T in (10) is a smoothing operator.

We now need to find the function $f(\boldsymbol{\rho}'; z')$ for a given g. In fact, as mentioned above, since scanning is involved, it is sufficient to recover only $f(0; 0)$, i.e. the value of the object at the confocal point. Complete reconstruction of f can then be achieved by repeating this procedure at each scanning position. In order to solve the Fredholm equation (11) we consider its singular system, given by the solutions of equations (3).

The adjoint $\boldsymbol{A}^*$ of $\boldsymbol{A}$ is given by

$$(\boldsymbol{A}^* g)(\boldsymbol{\rho}; z) = W(\boldsymbol{\rho}; z) \int W(|\boldsymbol{\rho} - \boldsymbol{\rho}'|; z) \, g(\boldsymbol{\rho}') \, \mathrm{d}\boldsymbol{\rho}'. \tag{21}$$

As explained above, the singular system of $\boldsymbol{A}$ is found by numerical computation and we can then reconstruct the object on the optical axis using the relations

$$f(0; 0) = \int M(\boldsymbol{\rho}') g(\boldsymbol{\rho}') \, \mathrm{d}\boldsymbol{\rho}', \tag{22}$$

where the optical mask is given by

$$M(\boldsymbol{\rho}) = \sum_{k=0}^{K-1} \frac{1}{\alpha_k} u_k(0; 0) v_k(\boldsymbol{\rho}), \tag{23}$$

where the series is truncated after K terms. This has the form of an oscillating ring system—see figure 1—and thus the integration in (22) requires the subtraction of some areas of the image from the rest.

In fluorescence microscopy we have no phase information and so we use a mask which both transmits and reflects. Two integrating detectors and an electronic subtractor process the transmitted and reflected components. The mask is made elliptical, to be placed at 45° to the optical axis and so present a circular cross-section to the incident light. A schematic diagram of this arrangement is shown in figure 2.

The image-plane mask may be conveniently fabricated as a 'binary-coded' version of the calculated continuous mask with aluminium rings deposited on a silica flat. The binary ring pattern of the mask is devised to emulate the continuous profile of the calculated mask with sufficient accuracy to preserve the resolving power of the microscope while still being easy to manufacture [9]. A diagram of the mask is shown in figure 3.

First images of a field of 100 nm diameter fluorescent calibration PVC spheres (Molecular Probes Ltd, Eugene, OR), are shown in figure 4 using an adapted commercial Bio-Rad MRC 600 scanning microscope in three imaging modalities, namely, type I (conventional

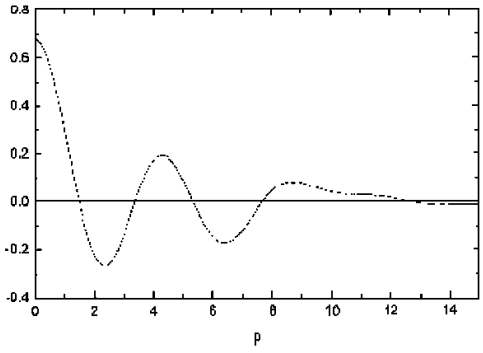

Figure 1. The calculated amplitude of the image-plane mask; ρ is the radial coordinate in optical units.

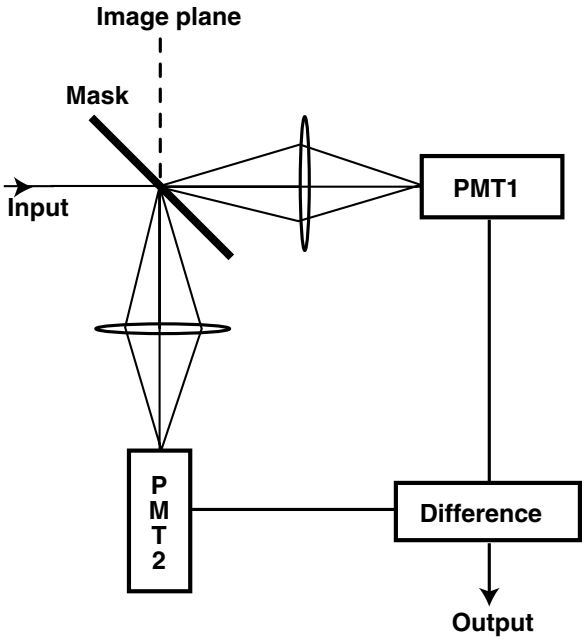

Figure 2. A schematic diagram of the image-plane mask arrangement.

microscopy), confocal and our image-plane mask scheme. A numerical aperture of 1.3 was used with 488 nm radiation. The leftmost sphere may be out of focus or at the edge of a scanning line. The insets show profiles taken across the two spheres near the bottom left corner. The progressive relative increase in resolution of the particles, from a full width of 12 pixels for the type I case down to 9 and 6 pixels, respectively, for the confocal and mask-detector cases is quite spectacular. However, absolute calibration is not yet available.

To obtain the results of figure 4 the collection and subtraction of the images from the mask was done using the in-built command language macros of the microscope. Further work is being done to implement these processes using an electronic subtraction circuit which will provide images much more quickly. When this has been completed we will be in a position to quantify accurately the resolution in absolute terms. We may then investigate the limits

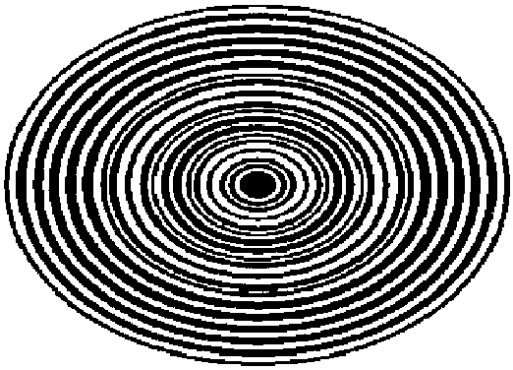

Figure 3. Binary realization of the image-plane mask.

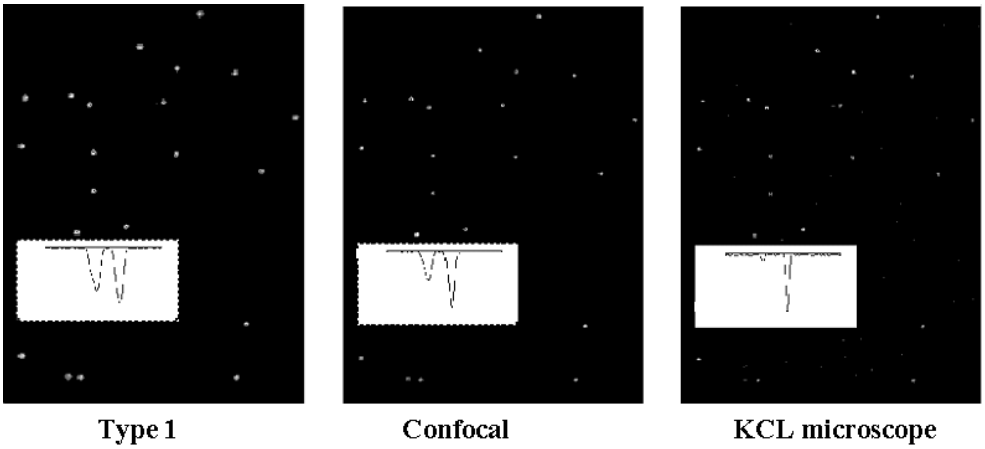

Figure 4. Images of 100 nm PVC calibration spheres.

of application of the method to the accurate determination of particle size and to study, for example, the effects of hydration and other microscopic details of interest.

Acknowledgments

We have been supported in earlier phases of this research programme by the NATO Scientific Affairs Division, the US Army and the UK Engineering and Physical Sciences Research Council and we are grateful to the Royal Society for a visiting Fellowship for Shi-Hong Jiang. We have also had help and encouragement from Andrew Dixon and support for a CASE student, Gerard Hester, from his company, Bio-Rad Sciences Ltd. We are pleased to acknowledge valuable collaboration with Mark Shipman and Ken Howard of University College, London, with the use of their MRC 600 microscope. Much of the original experimental work leading to these applications is published in the recent King's College PhD thesis of Dr Ulli Brand [10]. The work is currently partly supported by the European Union 'Super Laser Array Memory' Project.

References

[1] Wilson T and Sheppard C 1984 *Theory and Practice of Scanning Optical Microscopy* (London: Academic)

[2] Bertero M and Pike E R 1993 Signal processing for linear instrumental systems with noise: a general theory with illustrations from optical imaging and light scattering problems *Handbook of Statistics* vol 10, ed N K Bose and C R Rao (Amsterdam: Elsevier) pp 1–46

[3] Akduman I, Brand U, Grochmalicki J, Hester G and Pike E R 1998 Superresolving masks for incoherent high-numerical-aperture scanning microscopy in three dimensions *J. Opt. Soc. Am.* A **15** 2275–87

[4] Creffield C E, Klepfish E G, Pike E R and Sarkar S 1995 Spectral weight function for the half-filled Hubbard model: a singular value decomposition approach *Phys. Rev. Lett.* **75** 517–20

[5] Marchaud F B T, de Villiers G D and Pike E R 2001 Generalized Gaussian quadrature applied to an inverse problem in antenna theory *Inverse Problems* **17** 1163–79

[6] de Villiers G, McNally B and Pike E R 1999 Positive solutions to linear inverse problems *Inverse Problems* **15** 615–35

[7] Bertero M, Boccacci P, Davies R E, Malfanti F, Pike E R and Walker J G 1992 Superresolution in confocal scanning microscopy: IV. Theory of data inversion by the use of optical masks *Inverse Problems* **8** 1–23

[8] Ignatowsky V S 1921 Diffraction by an objective lens with arbitrary aperture *Trans. Opt. Inst. Petrograd* **1** 1–36 (in Russian)

[9] Grochmalicki J, Pike E R, Walker J G, Bertero M, Boccacci P and Davies R E 1993 Superresolving masks for incoherent scanning microscopy *J. Opt. Soc. Am.* A **10** 1074–7

[10] Brand U 2000 Optical data processing in high-numerical-aperture imaging *PhD Thesis* King's College, London